3 Biotech (2023) 13:38
https://doi.org/10.1007/s13205-022-03445-3

ORIGINAL ARTICLE

Development of 9-(*N*-arylmethylamino) congeners of noscapine: the microtubule targeting drugs for the management of breast cancer

Pratyush Pragyandipta[1] · Manas Ranjan Naik[2] · Banajit Bastia[1] · Pradeep Kumar Naik[1]

Received: 9 September 2022 / Accepted: 17 December 2022

Abstract

Noscapine is a natural lead molecule with anticancer activity at a higher concentrations. So, there is an urge for the development of more potent derivatives of noscapine. In this study, we have approached for development of 9-*N*-arylmethylamino derivatives of noscapine that kills cancer cells without affecting the normal cells. They were designed by substituting *N*-aryl methyl pharmacophore at the C-9 position and screened out top-ranked three derivatives **13a-c** using molecular docking. Further, their theoretical free energy of binding with tubulin was calculated followed by chemical synthesis and experimental validation. In vitro antiproliferative activity of noscapine and its 9-*N*-arylmethylamino derivatives (**13a-c**) was carried out using MCF-7 (a triple receptors positive) and MDA-MB-231 (a triple receptor negative) breast cancer cell lines. Further, cytotoxicity to normal cells was examined using human embryonic kidney cells (HEK cells). Inhibition to cell cycle progression and induction of apoptosis was monitored using FACS. The binding of noscapine and **13a-c** with tubulin was examined using fluorescence quenching assay. The 9-*N*-arylmethylamino derivatives of noscapine (**13a-c**) were found to inhibit the proliferation of cancer cells at a much lower concentration (IC_{50} values range between 9.1 to 47.3 µM) compared to noscapine (IC_{50} value is 45.8–59.3 µM). Surprisingly, the proliferation of HEK cells was not inhibited even at a concentration of 100 µM (cytotoxicity is < 5%). These derivatives induced apoptosis by arresting cells at G2/M-phase and also bind to tubulin. The 9-(*N*-arylmethylamino) noscapinoids have the potential to be a novel therapeutic agent for the treatment of breast cancer.

Keywords Anticancer drug · Drug discovery · 9-(*N*-arylmethylamino) derivatives · Tubulin · Microtubules

Introduction

The plant alkaloid noscapine has been administered orally as a safe antitussive drug for over 40 years. It is non-sedative, non-narcotic, and lacks respiratory-depressant without causing exhilaration or dependency (Dahlström et al. 1982; Karlsson et al. 1990). Noscapine was discovered to bind tubulin and regulate its dynamic instability. As a result, it inhibits cell cycle progression in dividing cancer cells and normal cells during the mitotic phase (Ye et al. 1998; Landen et al. 2002). However, cancer cells fail to arrest mitosis for a long duration due to their compromised cell cycle checkpoints and undergo apoptosis. In contrast, the arrested normal cells resume mitosis after drug removal (Zhou et al. 2002; Aneja et al. 2007a). More importantly unlike other microtubule targeting drugs like vinca alkaloids and taxanes, noscapine has several advantages like: (a) effective against wide range of cancer cells including the drug resistance ones (Zhou et al. 2002, 2006; Aneja et al. 2007a; Ke et al. 2000); (b) it is poor candidate for drug pumps (poly glycoproteins and multidrug resistance-related proteins), hence chances of developing resistance is minimum (Zhou et al. 2006), (c) when tested in nude mice it suppressed the growth of murine melanoma, glioblastoma, lymphoma and human breast tumours showing no toxicity to normal highly dividing cells and postmitotic cells like neurons (Zhou et al. 2002, 2006; Aneja et al. 2007a; Ke et al. 2000), (d) no sign of hindrance to primary humoral and cellular responses in mice (Ye et al. 1998; Ke et al. 2000; Krishna and Mayer 2000), (e) it does not cause measurable immunological and neurological toxicity in mice (Aneja et al. 2007a, 2010;

✉ Pradeep Kumar Naik
pknaik1973@gmail.com; pknaik1973@suniv.ac.in

[1] Centre of Excellence in Natural Products and Therapeutics, Department of Biotechnology and Bioinformatics, Sambalpur University, Jyoti Vihar, Burla, Sambalpur, Odisha 768019, India

[2] Department of Pharmacology, SLN Medical College Koraput, Koraput, Odisha 464020, India

Published online: 09 January 2023

Landen et al. 2004), (f) it is orally administered as opposed to other anti-MT drugs that require peritoneal injections or intravenous infusions with a risk of anaphylactic reactions (Aneja et al. 2007a), (g) it has a mean bioavailability of ~ 30 to 32 percent over a dose range of 10–300 mg/kg in mice (Jensen et al. 1992; Aneja et al. 2007b).

Noscapine is effective against a wide range of cancer cells at high micromolar ranges, so there is an urge to develop more potent derivatives of noscapine. Initially, several derivatives were being developed and synthesized based on hit and trial efforts, but very few molecules showed improved efficacy than the parent molecule noscapine (Zhou et al. 2003; Aneja et al. 2006a, b; Mishra et al. 2011). From an ongoing quest to improve our therapeutic arsenal, we have developed a battery of derivatives by modification of its scaffolds and demonstrated to have high tubulin binding and anti-tumor activity compared to noscapine without any debilitating toxicities (Manchukonda et al. 2012, 2013, 2014; Santoshi et al. 2011, 2015; Naik et al. 2011a, 2012). While several synthesized derivatives of noscapinoids showed promising in vitro activity against a panel of breast tumor cell lines, the antiproliferative activity comes to be in higher concentration ($IC_{50} > 20$ μM). Therefore, the status of research in India and internationally reflects an urgent need to take up further optimization of noscapine towards developing novel and more promising derivatives. In this study, we approach to develop 9-*N*-arylmethylamino noscapinoids by functionalizing the C-9 position of the scaffold structure of noscapine with Schiff base complex consisting of alkyl or arylalkyl units. This is because the Schiff bases (imine group containing pharmacophore) were reported to have anticancer properties (Adams et al. 2013; Bhat et al. 2013). Thus, there is a chance to increase the anticancer activity of noscapinoids. The 9-(N-arylmethylamino) noscapinoids revealed better binding affinity with tubulin, dramatically reduced cancer cell growth, arrested the cell cycle at G2/M phase and triggered apoptosis.

Materials and methods

Preparation and optimization of crystal structure of tubulin

The co-crystal structure of tubulin heterodimer (PDB ID: 6Y6D) was downloaded from protein data bank. A complex consisting of both 'A' and 'B' chains of the protein was acquired after a manual inspection and considered for molecular docking of noscapine and its derivatives. It is reported that noscapine and its derivatives were bound at the interface of both α- and β- tubulin (Naik et al. 2011b). Though the structure was obtained at a higher resolution of 2.20 Å using X-ray diffraction (Oliva et al. 2020), it has specific errors. A multistep protein preparation wizard (PP wizard) (Schrödinger, Inc., NY) was employed to preprocess the PDB structure, obtain the tubulin αβ-heterodimer and added missing hydrogen atoms. The Prime software (Schrödinger, Inc., NY) was used for the prediction of missing side chain atoms of the amino acids and repaired. The PP wizard was used to treat the metal magnesium to break bonds to neighbouring atoms and the correct formal charges to it was assigned by OPLS 2005 force field. Finally, the PP wizard was used to optimize hydrogen-bonding networks followed by energy minimization of the co-complex structure of tubulin-amino noscapine.

Rational design of 9-N-arylalkylamino derivatives of noscapine

Among the several derivatives of noscapine developed earlier, the derivatives developed by substitution of functional groups at C-9 position (e.g. fluoro, chloro, bromo, iodo, nitro, amino and azido) were found to have enhanced anticancer activity compared to the parent compound, noscapine. Out of them 9-amino-noscapine is the most prominent one. Later studies predicted that further functionalization of groups at C-9 position of isoquinoline ring system could be the choice to tune anticancer activity profile of noscapine. Schiff bases (imine group containing pharmacophore) are reported as antibacterial, anti-inflammatory, antioxidant and anticancer properties (Adams et al. 2013; Bhat et al. 2013). As an example, Schiff base obtained from coumarin and pyrazole aldehyde has been tested against cancer cell lines and showed mild anticancer activity (Ali et al. 2013). Physiological activities attributed to Schiff bases are due to predictable C=N functionality. Inspired by the potential applications of Schiff base analogues in pharmaceutical industry, and continuing our efforts on the development of newer and potent noscapine analogues, we have appended Schiff base complex with alkyl or arylalkyl units onto the noscapine scaffold. Initially, we developed a series of 9-(*N*-arylalkylamino) noscapinoids in silico as depicted in Fig. 1 followed by screening a panel of the most potent compounds using molecular docking and predictive binding free energy.

Preparation and optimization of the chemical structure of noscapinoids

Molecular structures of noscapine (PubChem ID: 275,196) and its derivatives (Fig. 2) that had been reported earlier (Aneja et al. 2006b; Santoshi et al. 2011, 2015; Manchukonda et al. 2013; Naik et al. 2011a) and the newly designed 9-(*N*-arylalkylamino) noscapinoids (Fig. 1) were built by ChemDraw (v19.0) and were imported into Maestro (Schrödinger, Inc., NY). The molecules were optimized by energy minimization using Macromodel (Schrödinger,

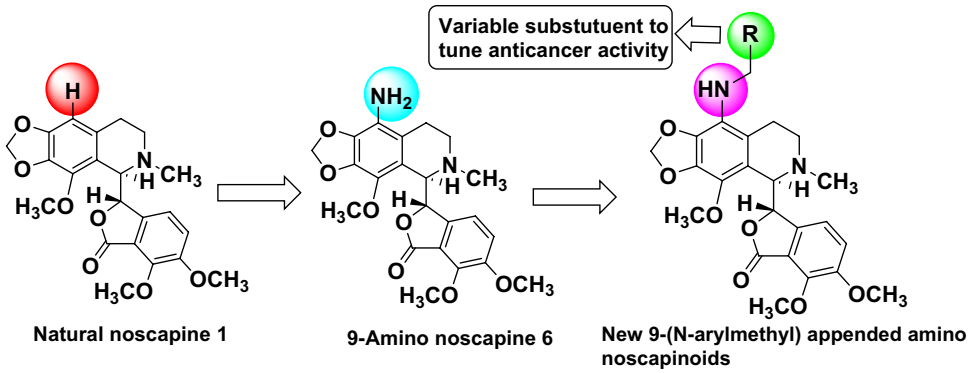

Fig. 1 In silico modification of noscapine scaffold with alkyl or arylalkyl units at the C-9 position to form a series of 9-(*N*-arylalkylamino) noscapinoids

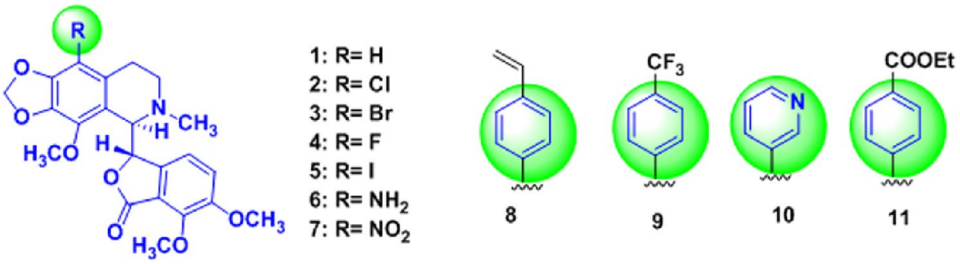

Fig. 2 Molecular structures of previously reported noscapine derivatives that have experimentally proven to bind tubulin with known binding free energy (Table 1) and used as training test molecules for LIE-SGB model building

Inc., NY) and OPLS 2005 force field. Polak-Ribiere Conjugate Gradient (PRCG) algorithm with an energy gradient of 0.01 kcal/mol and simulation of 1000 steps was used. Jaguar (version 17.4, Schrödinger, LLC) was used to optimize ligand geometry with a basic set of 3-21G* (Binkley et al. 1980; Gordon et al. 1982), using Becke's three-parameter exchange potential and the Lee–Yang–Parr correlation functional (B3LYP) (Lee et al. 1988; Becke 1993). Ligprep (Schrödinger, Inc., NY) was further employed to generate different conformations of the structures.

Molecular docking

Noscapine and its previously reported derivatives (Fig. 2) as well as 9-(*N*-arylalkylamino) derivatives (Fig. 1) were docked onto the binding site as reported earlier (Oliva et al. 2020). The noscapinoid binding site onto tubulin (PDB ID: 6Y6D) was specified by selecting the co-crystalized ligand, amino noscapine, as a reference molecule (Oliva et al. 2020). The Glide grid receptor generation algorithm was used to generate two grid boxes by choosing the co-crystal ligand amino-noscapine to specify the binding site. An inner grid box of size 12 Å × 12 Å × 12 Å was made at the centroid of the binding site indicating that each docked ligand's diameter midpoint must be present in the search space. Along with this box, an outer grid box was also formed with a size of ≤ 24 Å of the co-complexed amino noscapine specifying the volume in which the ligand's must restrain. The Glide XP method (Schrödinger, Inc., NY) was used to dock the molecules and their binding poses were evaluated using the GlideXP$_{Score}$ function (Friesner et al. 2004; Halgren et al. 2004). Protein atoms with precise partial charges less than or equal to 0.25 was used as a scaling factor and 0.4 for van der Waals radii. Out of the 10,000 poses assessed, 1000 were chosen using energy minimization (conjugate gradients), and the 30 structures with the lowest energy conformation were used to determine Glide docking score. The ten best conformations for each molecule were chosen, and the average docking score was calculated. Finally, the best three 9-(N-arylmethylamino) derivatives of noscapine, **13a-c**, (Fig. 3) from the library were screened out for theoretical calculation of free energy of binding, chemical synthesis, and experimental validation.

Theoretical calculation of free energy of binding of 13a-c with tubulin

A predictive model was developed based on linear interaction energy model (LIE) with a surface generalized Born (SGB) continuum solvation model (Zhou et al. 2001) to determine the free energy of binding ($\Delta G_{bind,pred}$) of the newly designed 9-(*N*-arylalkylamino) noscapinoids (**13a-c**) with tubulin. A training data set of noscapinoids (Fig. 2) with known experimental free energy of binding ($\Delta G_{bind,expt}$) was used and mapped with various predicted energy parameters such as van der Waals (U_{vdw}), coulombic (U_{coul}), reaction field (U_{rxn}) and cavity energy (U_{cav}) based on LIE model to develop the empirical prediction model. The $\Delta G_{bind,expt}$ of noscapinoids was calculated from their respective dissociation constant (K_d) values using the relation:

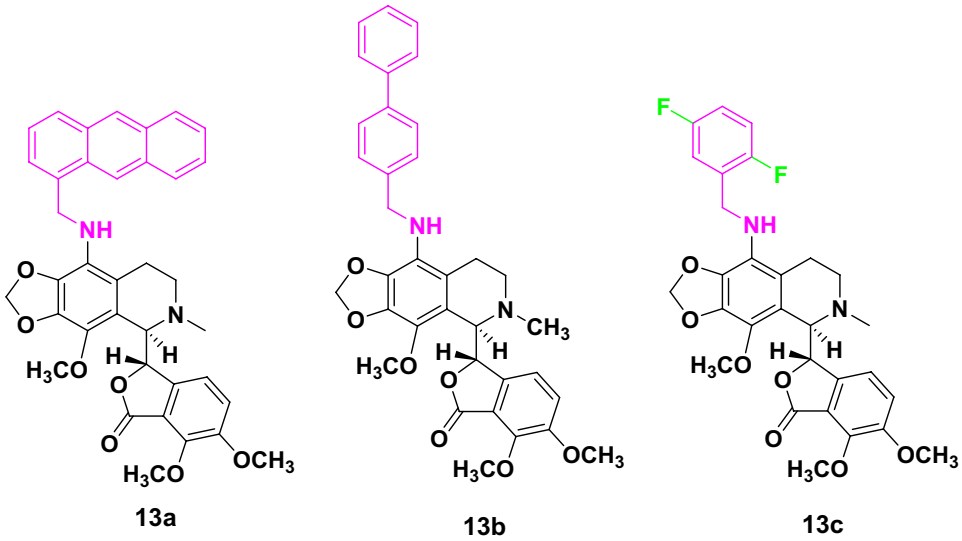

Fig. 3 Chemical structure of promising 9-(*N*-arylmethyl-amino) noscapinoids, **13a-c**, screened out with better binding affinity with tubulin

$$\Delta G_{\text{bind,pred}} = RT\ln Kd,$$

where R is the gaseous constant (0.001986 kcal/mol) and T is the temperature (298 K). Liaison programme (Schrödinger package) was used with the parameters set up as reported previously (Santoshi et al. 2015) to estimate the above energy parameters from the docked complexes of the noscapinoids based on Hybrid Monte Carlo simulation technique.

$$\Delta G_{\text{bind,pred}} = \alpha\left(\langle U^b_{vdw}\rangle - \langle U^f_{vdw}\rangle\right) + \beta\left(\langle U^b_{coul}\rangle - \langle U^f_{coul}\rangle\right) + \gamma\left(\langle U^b_{rxn}\rangle - \langle U^f_{rxn}\rangle\right) + \delta\left(\langle U^b_{cav}\rangle - \langle U^f_{cav}\rangle\right).$$

Here <> represents the ensemble average, b represents the bound form of the ligand, f represents the free form of the ligand, and α, β, γ and δ are the coefficients of the energy parameters. The values obtained for the four fitting parameters, α, β, γ and δ were 0.08446, − 0.00223, − 0.00872, and − 0.45601, respectively. The $\Delta G_{\text{bind,pred}}$ of the training set molecules based on the LIE-SGB model was very close to the $\Delta G_{\text{bind,pred}}$ (root mean square error was 0.243 kcal/mol). The accuracy of the prediction model can also be judged by the squared correlation coefficient (R^2) and analysis of variance (F value).

$$\nabla G_{\text{bind,pred}} = 0.08446\langle U_{\text{vdw}}\rangle - 0.00223\langle U_{\text{coul}}\rangle - 0.00872\langle U_{\text{rxn}}\rangle - 0.45601\langle U_{\text{cav}}\rangle$$
$$(n = 11,\ R^2 = 0.998,\ s = 0.243,\ F = 3742.6,\ P \le 0.001)$$

Because of high predictability, the LIE-SGB prediction model was used to predict the free energy of binding of the newly designed 9-(N-arylalkylamino) noscapinoids (**13a-c**).

Chemical synthesis of 9-(*N*-arylalkylamino) noscapinoids (13a-c)

Noscapine procured from Sigma-Aldrich was used as starting material to synthesize the 9-(*N*-arylalkylamino) noscapinoids (**13a-c**) through 2 reaction phases, such as (a) bromination of noscapine with aqueous HBr/Br_2-H_2O and (b) amination of noscapine with CuI, NaN_3, and L-Proline in DMSO (Naik et al. 2011a). In 15 ml of ethanol, the 9-amino-noscapine **6** solution (1.0 mmol) was refluxed with a number of substituted aromatic aldehydes (1.0 mmol). The solvent was evaporated under a vacuum until the reaction consumed all the starting material (as suggested by TLC). The crude residue was extracted using dichloromethane (2 × 15 ml) followed by washing in a brine solution. After being collected and passed through Na_2SO_4 bed, the organic layer was removed at a lower pressure. Chromatography of the crude residue was done using petroleum ether/ethyl acetate (7:3) as eluents over a triethylamine silica bed to give 9-(arylimino) derivatives of noscapine **12a-c** as solid compounds in high yields. Further, in the presence of sodium cyanoborohydride (1.2 mmol) in methanol (10 mL) for 4 h at room temperature the intermediate products **12a-c** (1.0 mmol) were reduced to get 9-(*N*-arylmethylamino) derivatives, **13a-c** as depicted in Reaction Scheme 1. NMR (^{1}H and ^{13}C), IR spectroscopy,

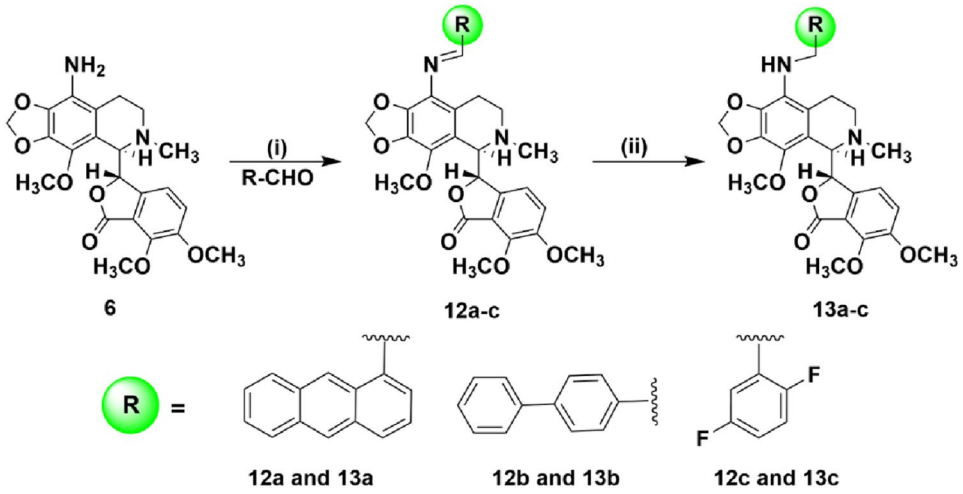

Reaction Scheme 1 Scheme 1 Chemical synthesis of screened out 9-(*N*-arylmethylamino) derivatives of noscapine 13a-c. Reaction Conditions: (i) RCHO, EtOH, Reflux, 24 h; (ii) NaCNBH3, Methanol, RT, 4 h. 9-amino-noscapine was transformed to 9-(arylimino) derivatives of noscapine 12a-c, which were subsequently reduced to 9-(*N*-arylmethylamino) derivatives of noscapine 13a-c

and mass (HRMS) spectrometry were used to characterize all intermediates and end products. The spectroscopy data of all the intermediates and final products are collated in the supplementary data (Supplementary data S1-S25).

Cancer cell lines and reagents

Human breast cancer cell lines (MCF-7 & MDA-MB-231) and normal human embryonic kidney cell line (HEK) was acquired from National Centre for Cell Science in Pune, Maharashtra, India. For experimental validation of **13a-c** stock solutions (100 mM) were prepared using DMSO (Dimethyl sulfoxide) and stored at 4 °C until further use. Cells were grown in DMEM (Dulbecco's modified Eagle medium) along with 10% fetal bovine serum (FBS; GIBCO) and 1% penicillin and streptomycin (Himedia) at 37 °C and 5% CO_2 with 95% humid conditions. Once the cells had attained 70–80% confluency, they were subcultured using trypsin–EDTA (0.25%) for further cellular assay.

Proliferation assay using breast cancer cells

About 5×10^3 number of MCF-7, MDA-MB-231, and normal human embryonic kidney (HEK) cell lines were plated in a 96 wells plate and treated with noscapine and its 9-(*N*-arylmethylamino) derivatives **13a-c** of varying concentrations (5–100 µM) for 72 h. Sulforhodamine B assay was used to determine the viability of cells. The plate's reading was taken in a microplate spectrophotometer (SPECTRAmax PLUS 384) at 564 nm wavelength. The IC_{50} value was calculated in Quest GraphTM IC_{50} Calculator (AAT Bioquest, Inc., Sunnyvale, CA, USA, https://www.aatbio.com/tools/IC50-calculator).

Cell cycle progression assay

The cell cycle progression due to the administration of 9-(*N*-arylmethylamino) derivatives of noscapine, **13a-c**, was analyzed as previously described (Pragyandipta et al. 2021). About 1×10^5 number of MDA-MB-231 breast cancer cells were cultured in a 6-well culture plate overnight and treated with IC_{50} concentrations of noscapine and its 9-(*N*-arylmethylamino) derivatives **13a-c**. The proportion of cells in each cell cycle stage was assessed using flow cytometry (BD FACS Aria-III) after 72 h of treatment. The experiment was done in triplicates.

Apoptosis assay

The induction of apoptosis was carried out as previously reported (Pragyandipta et al. 2021). In a 12 well culture plate around 3×10^4 MDA-MB-231 breast cancer cells were seeded, followed by treatment with IC_{50} concentrations of noscapine and its 9-(*N*-arylmethylamino) derivatives **13a-c** for 72 h and was analyzed by flow cytometer. The apoptotic cells were identified using the apoptosis detection kit (Sigma-Aldrich, USA), which contains FITC-conjugated streptavidin, biotin-conjugated Annexin V, and propidium iodide (PI). Viable cells (Annexin V−/PI−), early apoptotic cells (Annexin V+/PI−), late apoptotic/necrotic cells (Annexin V+/ PI+) and late necrotic cells (Annexin V−/PI+) were identified and determined their percentage.

Tubulin purification

Using two cycles of temperature and GTP-dependent polymerization and depolymerization tubulin was isolated from goat brain and purified by phosphocellulose chromatography as reported earlier (Panda et al. 2000; Hamel and Lin 1981). The purified tubulin was stored at − 86 °C for further use.

Tubulin binding assay

Along with PEM buffer (50 mM pipes, 3 mM $MgSO_4$, 1 mM EGTA, pH 6.8), the 9-(*N*-arylmethylamino) derivatives of noscapine, **13a-c** (25 µM) were incubated with tubulin (2 µM) at 35 °C in a water bath for 45 min. The emission range for the samples was 310–400 nm, and the excitation wavelength was 295 nm in a FlouroMax® 4 spectrofluorometer (Horiba Scientific, Edison, NJ).

Results

Molecular docking and theoretical binding energy calculation of 9-(*N*-arylmethylamino) derivatives of noscapine

Noscapine and its 9-(*N*-arylalkylamino) derivatives were docked onto the noscapinoid binding site of tubulin by selecting the co-crystalized compound, amino-noscapine, as a reference molecule using GlideXP algorithm. Our docking protocol also regenerated the identical geometry of the reference molecule's and mode of interaction as observed in the co-crystal structure. This is the alternative method to validate the docking protocol reported earlier in the absence of the co-crystalized protein structure and ligands (Bhardwaj et al. 2022; Sharma et al. 2021). Further, we have used up to 10 different conformations of each ligand to dock onto the binding site and calculated the average docking score since the ligands' bioactive conformations were unknown. Others have utilized similar method to decipher the mode of interaction of ligands with the protein in the absence of bioactive conformation (Bhardwaj et al. 2022; Sharma et al. 2021). In comparison to the lead molecule, noscapine with a docking score -2.746 ± 0.539 kcal/mol, all 9-(*N*-arylalkylamino) derivatives of noscapine revealed enhanced docking score (ranging from − 3.752 to − 5.298 kcal/mol). Finally, three top-ranked derivatives **13a-c** (Fig. 3) based on the improved docking score (− 4.728, − 4.765 and − 5.298 kcal/mol) compared to noscapine (Table 1) were selected for the theoretical calculation of free energy of binding based on LIE-SGB prediction model. The predicted free energy of binding of 9-(*N*-arylalkylamino) derivatives of noscapine (− 6.467 kcal/mol for **13a**, − 7.077 kcal/mol for **13b** and − 7.468 kcal/mol for **13c**, respectively) were found to be significantly higher compared to the noscapine (free energy of binding is − 4.845 kcal/mol) (Table 1). Noscapine and its 9-(*N*-arylalkylamino) derivatives fit nicely inside the binding site and were analyzed for the interaction pattern using Ligplot (Figs. 4 and 5).

Ligplot analysis revealed the binding modalities of noscapine and its 9-(N-arylalkylamino) derivatives **13a-c**, with the amino acids of the binding site (Fig. 5a–d). The binding site amino acids form three hydrogen bonds (dashed line) with the most promising derivative (**13c**). In particular, the side-chain nitrogen atoms of Gln B247 (bond length

Table 1 Liaison (Schrödinger, Inc., NY) was used to calculate Glide XP_{score} along with other parameters like van der Waals energy (U_{vdw}), Columbic energy (U_{coul}), reaction energy (U_{rxn}) and cavity energy (U_{cav}) for noscapine and its 9-(N-arylalkylamino) derivatives (**13a-c**)

Ligand	$GlideXP_{score}$ (kcal/mol)	$<U_{vdw}>$ (kcal/mol)	$<U_{coul}>$ (kcal/mol)	$<U_{rxn}>$ (kcal/mol)	$<U_{cav}>$ (kcal/mol)	$\Delta G_{bind,expt}$ (kcal/mol)	$\Delta G_{bind,pred}$ (kcal/mol)
1	− 2.746 ± 0.539	− 43.43	− 202.48	115.81	1.357	− 4.802	− 4.845
2	− 3.052 ± 0.641	− 47.29	− 331.08	123.31	4.171	− 6.725	− 6.704
3	− 3.689 ± 0.807	− 45.79	− 368.38	148.71	3.282	− 6.812	− 6.177
4	− 3.518 ± 1.093	− 52.35	− 356.08	172.51	4.622	− 5.210	− 5.764
5	− 3.736 ± 1.117	− 54.98	− 273.98	129.31	2.177	− 6.932	− 6.153
6	− 4.188 ± 0.643	− 47.73	− 177.58	129.01	1.028	− 5.956	− 5.229
7	− 3.984 ± 1.237	− 38.68	− 332.18	183.51	1.539	− 6.231	− 6.234
8	− 3.990 ± 0.838	− 51.86	− 278.18	102.11	4.359	− 6.745	− 6.638
9	− 3.721 ± 0.904	− 33.76	− 324.78	152.31	3.841	− 5.783	− 5.207
10	− 3.731 ± 0.940	− 45.72	− 471.48	152.61	3.743	− 5.673	− 5.848
11	− 3.926 ± 1.069	− 42.98	− 267.88	129.71	3.539	− 5.518	− 5.778
13a	− 4.728 ± 0.919	− 52.63	− 280.98	145.41	3.027	Nd	− 6.467
13b	− 4.765 ± 1.626	− 50.01	− 305.38	149.51	4.891	Nd	− 7.077
13c	− 5.298 ± 1.229	− 56.2	− 274.78	140.61	4.622	Nd	− 7.468

Based on the LIE-SGB prediction model, the predicted binding free energy ($\Delta G_{bind,pred}$) was determined. All the newly synthesized 9-(*N*-arylalkylamino) derivatives **13a-c** showed better $\Delta G_{bind,pred}$ compared to the lead molecule, noscapine

The energy terms $<U_{vdw}>$, $<U_{coul}>$, $<U_{rxn}>$ and $<U_{cav}>$ indicate the ensemble average energy calculated due to the difference between bound and free state of the ligands and its environment. Experimental ΔG_{bind} was calculated experimentally using the dissociation constant (K_d value) using the equation: $\Delta G_{bind} = RT \ln K_d$ where $T = 298$ K and $R = 0.00199$ (kcal/mol K). *Nd* not determined

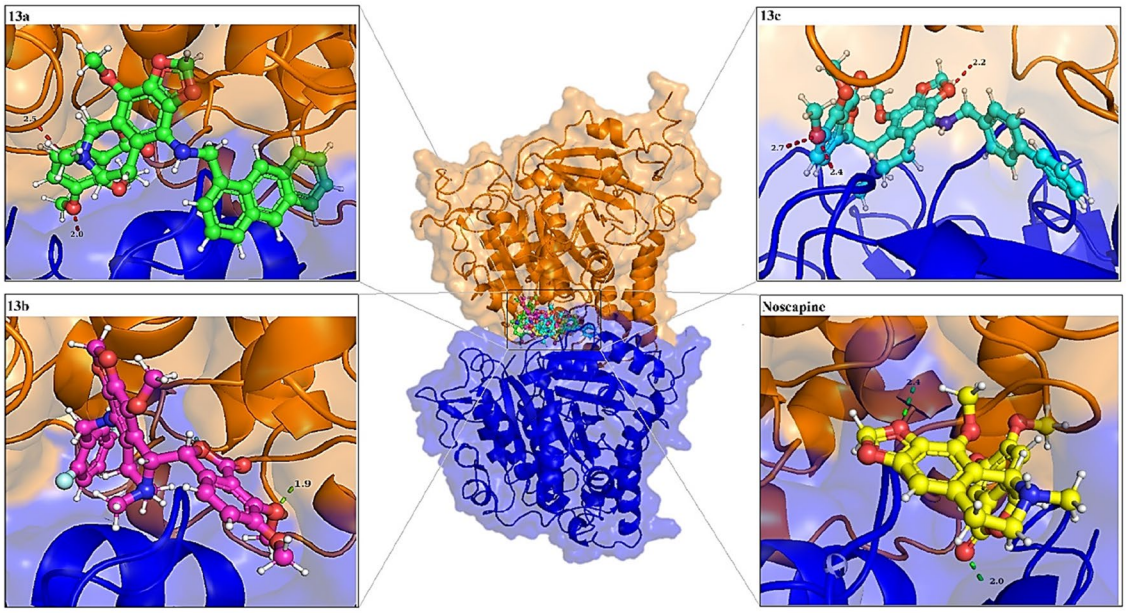

Fig. 4 Noscapine and its derivatives **13a-c** revealed well accommodation inside the binding pocket. α-tubulin is labeled with brown while β-tubulin is labeled with blue color. The dashed lines are the hydrogen bonds. A macromodel surface represents the binding domain

3.13 Å), Gln A15 (bond length 3.27 Å) and Thr A223 (bond length 2.83 Å), formed hydrogen bonds with the oxygen atoms O4, N1, and O6, respectively of **13c** (Fig. 5d). In contrary the derivative **13b** forms 1 hydrogen bonds with the binding site amino acids Met B325 (Fig. 5c) while derivative **13a** forms only two hydrogen bonds with the binding site amino acids Arg B48 (Fig. 5b). Only two hydrogen bonds were generated by the lead molecule, noscapine, with the binding site amino acids Gln B247 & Val B355 (Fig. 5a). The binding of noscapine and its derivatives **13a-c** to the binding site amino acids was also aided by a series of hydrophobic interactions (Supplementary Table S26–S29). To gain more information about the interaction of noscapine and its 9-(*N*-arylalkylamino) derivatives with the binding site amino acids, we have calculated the van der Walls (E_{vdw}) and electrostatic (E_{ele}) energy contribution of the residues within 12 Å of docked ligands. The binding site amino acids showed a significant contribution of E_{vdw} and E_{ele} energy with the docked ligands (Fig. 6). Specifically, two amino acids, Gln B247 and Gln A176 have an appreciable E_{ele} energy contribution (≤ -3 kcal/mol) with the binding of **13c**. In contrast, a single amino acid Met B325 and Gln B247 have an appreciable E_{ele} energy contribution (≤ -3 kcal/mol) with the binding of **13b** and **13a,** respectively. Similarly, a good number of amino acids were involved in van der Waals interaction with the docked ligands. Specifically, 5 amino acids (Glu B330, Asp B329, Glu B327, Glu A207 and Glu A220), 5 amino acids (Glu B330, Asp B329, Glu B327, Glu A220 and Glu A207), 3 amino acids (Glu B330, Asp B329 and Glu A207), and 4 amino acids (Glu B330, Asp B329, Glu B327 and Glu A220) form van der Waals interaction with **13c, 13b, 13a** and **Noscapine**, respectively. The difference in the interaction profile is due to the substitution of different functional groups in the scaffold structure of noscapine.

9-(*N*-arylmethylamino)-13a-c derivatives inhibited the proliferation of breast cancer cell line

Two human breast cancer cell lines, MCF-7 (estrogen- and progesterone-receptor positive) and MDA-MB-231 (estrogen- and progesterone- receptor negative) were treated with Noscapine and its 9-(*N*-arylalkylamino) derivatives **13a-c** to investigate their antiproliferative activity. It revealed that the noscapinoids (**13a-c**) hindered the cancer cell proliferation at lower dosages than the parent molecule noscapine (Fig. 7). When treated against MCF-7 cell line, the noscapine and its derivatives, **13a-c** showed IC_{50} value of 45.8 µM, 37.2 µM, 30.9 µM and 19.4 µM, respectively. In comparison, in the case of MDA-MB-231 cell line, the IC_{50} values were 59.3 µM, 47.3 µM, 33.7 µM, and 24.1 µM for noscapine and its derivatives, **13a-c** respectively (Table 2). The difference in IC_{50} values for both cell lines indicates that the

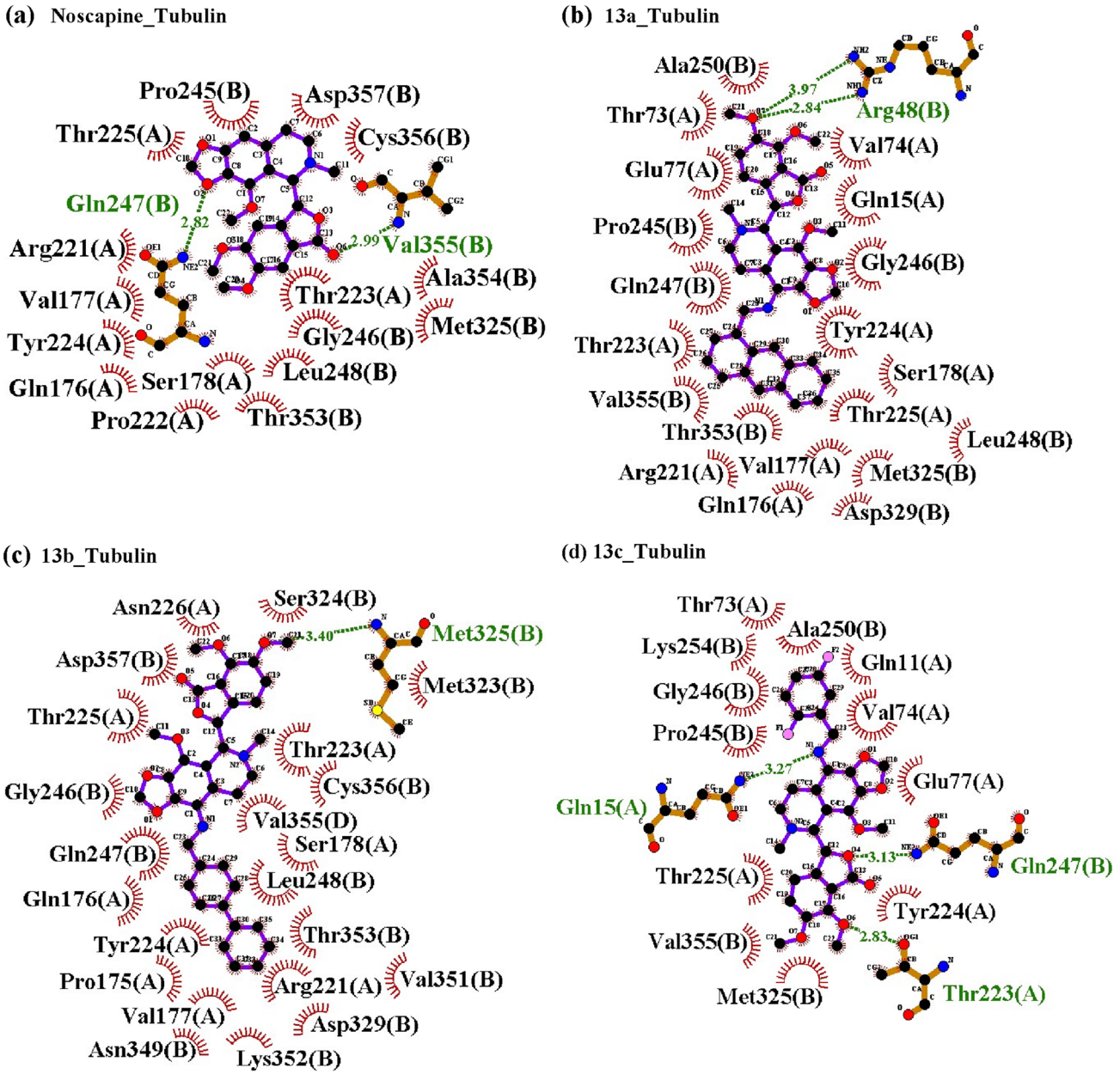

Fig. 5 Ligand protein interaction (ligplot) analysis revealed the association of tubulin binding site amino acids with **a** Noscapine, **b 13a**, **c 13b** and **d 13c**. Dashed lines indicate hydrogen bonds, while numerals reflect length of hydrogen bond in Å. The radial spoke arcs represent the hydrophobic molecular interactions

susceptibility of cancer cells to noscapine and its derivatives, **13a-c** is cell type-dependent. Additionally, we have also evaluated the toxicity profile of noscapine and its derivatives (**13a-c**) to normal healthy dividing cells by using HEK. When the normal cells were treated with noscapine and its derivatives, **13a-c** at a high concentration of 100 µM the antiproliferative activity was found to be < 5% suggesting extremely low or no toxicity to normal healthy cells (Fig. 8).

9-(*N*-arylmethylamino) derivatives 13a-c induced apoptosis to cancer cells

The induction of apoptosis in breast cancer cells after treatment with 9-(N-arylmethylamino) derivatives **13a-c** was done by FACS. During apoptosis, the translocation of phosphatidylserine to the cell membrane's outer leaflet was detected by annexin V and the propidium iodide to DNA. Cells were treated with IC_{50} concentrations of noscapine

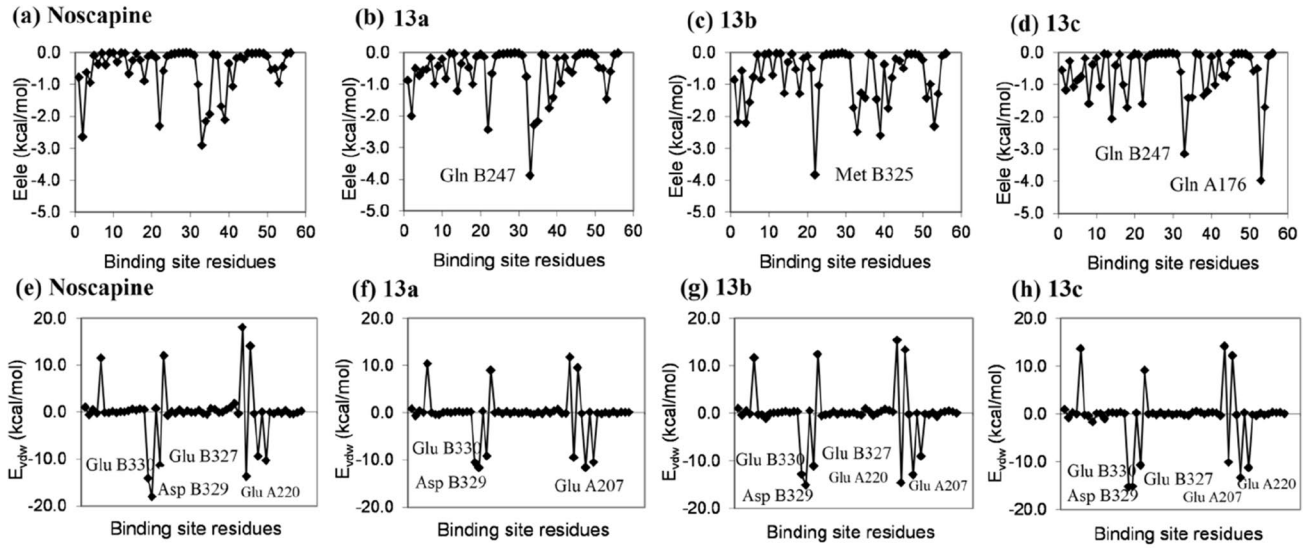

Fig. 6 Interaction profile of binding site amino acids with the docked noscapine and its 9-(*N*-arylalkylamino) derivatives (**13a-c**). Only the electrostatic (E_{ele}) and van der Walls (E_{vdw}) energy contribution of residues within the 12 Å diameter of docked ligands are being considered. It clearly shows that binding site residues contribute differently to the electrostatic and van der Walls binding energy with docked ligands. For the E_{ele} energy contribution, only the amino acids contributing energy ≤ -3 kcal/mol were labeled, whereas in case of E_{vdw} energy contribution, the amino acids having energy contribution of ≤ -10 kcal/mol were labeled

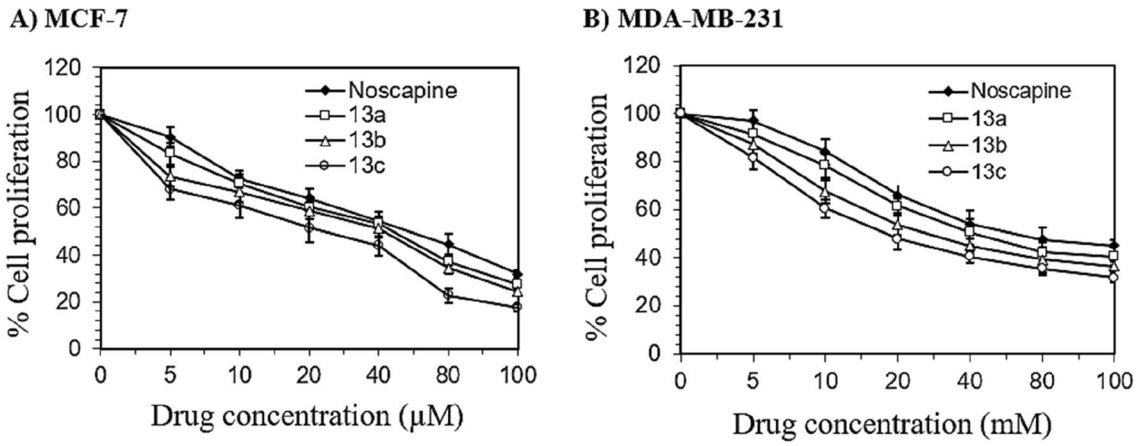

Fig. 7 Growth of **A** MCF-7 and **B** MDA-MB-231 cancer cells when treated against escalating concentration of noscapine & **13a-c** derivatives for 72 h was found to be dramatically inhibited. The value is represented as mean (±) standard deviation

Table 2 Noscapine and its derivatives' (**13a-c**) IC_{50} values when treated against MCF-7 and MDA-MB-231 cell lines

Breast cancer cell lines	IC_{50} (μM)			
	Noscapine	**13a**	**13b**	**13c**
MCF-7	45.8 ± 4.2	37.2 ± 3.2	30.9 ± 2.5	19.4 ± 1.9
MDAMB-231	59.3 ± 4.6	47.3 ± 3.5	33.7 ± 2.5	24.1 ± 2.4

Compared to noscapine, these molecules showed enhanced anti-proliferative efficacy

and its derivatives **13a-c** for 72 h against MDA-MB-231 cell line to determine the percentage of early and late apoptotic cells. A flow cytometry analysis of apoptotic cells is shown in Fig. 9. In control, there were very few early (3.5%) and late (2.0%) apoptotic cells, and were considered background cell death due to normal necrosis of cells. In contrast, with treatments of noscapine and its derivatives **13a-c**, the percentages of early apoptotic cells were found to be 20%, 40%, 35%, and 30%, while the late apoptotic cells were found to be 28%, 36%, 43%, and 50% which is more than that of the untreated cells (Table 3).

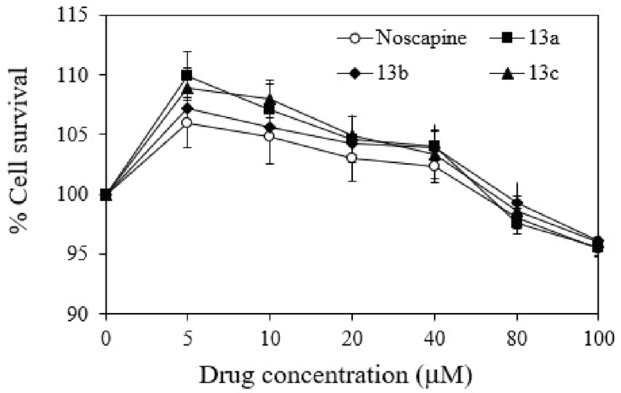

Fig. 8 Around < 5% cell death was revealed when normal human embryonic kidney cells (HEK) were treated with noscapine and its derivatives **13a-c** for 72 h. Each value is the average of three separate experiments

Inhibition of cell cycle progression by noscapine and its derivatives, 13a-c

The impact of noscapine and its 9-(*N*-arylmethylamino) derivatives **13a-c** (with the treatment of IC_{50} concentration) in cell cycle progression of MDA-MB-231 cells is illustrated in Fig. 10. The deposition of fluorescently tagged DNA in the presence of **13a-c** reveals that cell cycle progression has been disrupted. The presence of 2 N DNA marks the G1 phase, while 4 N DNA accumulation reveals the cells are at G2/M phase. DNA accumulation between 2 N & 4 N peaks indicates the cells are in S phase and in case there is less than 2 N DNA, it signifies the apoptotic cells with DNA degradation. The cell cycle profile of the MDA-MB-231 cell was significantly inhibited after 72 h of treatment with IC_{50} concentrations of noscapine and its derivatives (**13a-c**) (Table 4). A large deposition of cells were seen in the G2/M phase followed by emergence of hypodiploid DNA content peak (sub-G1) indicating apoptotic cells.

9-(N-arylmethylamino) derivatives of noscapine 13a-c were found to bind tubulin

Due to the inclusion of numerous tryptophan amino acids, tubulin is auto fluorescent in nature. Hence a drop in emission fluorescence associated with ligand binding owing to conformational changes might be beneficial in monitoring ligand binding. In the presence of 9-(*N*-arylmethylamino) derivatives of noscapine **13a-c** (25 μM), fluorescence intensity was reduced by 38%, 17.39%, and 25.47%, respectively, indicating these compounds bind to tubulin and altered its conformation (Fig. 11).

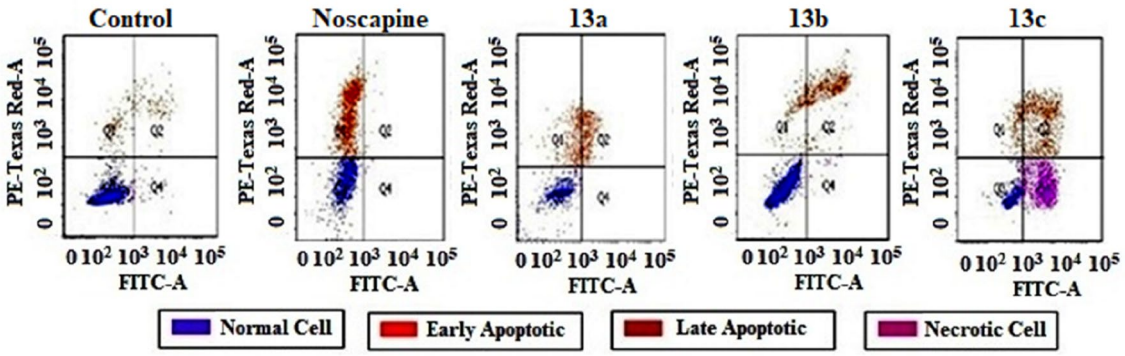

Fig. 9 Noscapine and its 9-(*N*-arylmethylamino) derivatives **13a-c** were treated against the MDA-MB-231 cell line and induction of apoptosis was assessed by flow cytometry and compared to non-treated cells. The fluorescent dye, propidium iodide (PI) was used in combination with the Alexa Fluor 488 conjugate of Annexin-V to discern between three sub-populations: PI-positive and Alexa Fluor 488-positive, indicating late apoptotic cells (PI+, Alexa Fluor 488+), PI-negative and Alexa Fluor 488-negative, indicating viable cells (PI-, Alexa Fluor 488-), PI-negative and Alexa Fluor 488-positive, indicating early apoptotic cells (PI-, Alexa Fluor 488+)

Table 3 The percentage of early apoptotic (Q1), late apoptotic (Q2), viable (Q3), and necrotic (Q4) was determined by Flow Cytometry

Viability/apoptotic	Control (%)	Noscapine (%)	**13a** (%)	**13b** (%)	**13c** (%)
Viable cell	94	40	10	15	10
Early apoptotic	2	20	40	35	30
Late apoptotic	4	28	36	43	50
Necrotic	0	0	10	10	10

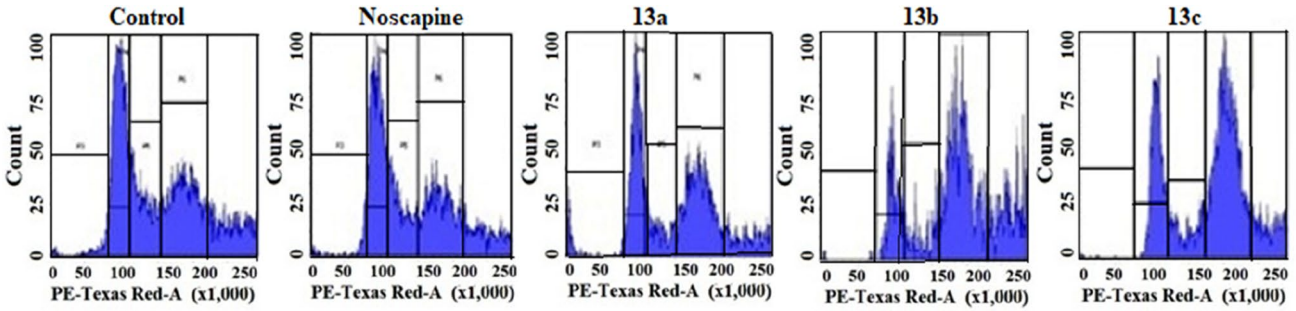

Fig. 10 Noscapine and its 9-(N-arylmethylamino) derivatives, **13a-c** disrupt cell cycle progression during the G2/M phase, followed by the emergence of a hypodiploid (sub-G1) DNA peak, suggesting apoptotic cells

Table 4 Effects of noscapine and its derivatives **13a-c** on cell cycle progression when treated with IC_{50} concentration using MDA-MB-231 cells for 72 h

	72 h			
	Sub-G_1	G_0/G_1	S	G_2/M
Control	0.8	20.9	23.6	10.9
Noscapine	4.8	16.9	14.8	18.1
13a	7.8	14.2	9.4	18.5
13b	9.0	15	8.8	37.2
13c	10.5	27.1	9.6	45.1

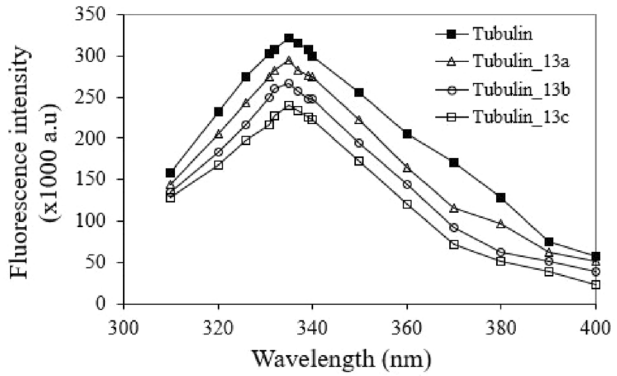

Fig. 11 9-(*N*-arylmethylamino) derivatives of noscapine **13a-c** reduce the fluorescence intensity of tubulin. The purified tubulin (2.0 µM) was incubated with **13a-c** (25 µM) and emission spectra (310–400 nm) were monitored. The inherent tubulin fluorescence emission intensity was quenched in presence of 9-(N-arylmethylamino) derivatives of noscapine **13a-c**, suggesting that they bind to tubulin

Discussion

9-(*N*-arylmethylamino) derivatives of noscapine have been investigated extensively for their anticancer activities. Schiff base obtained from coumarin and pyrazole aldehyde has been tested against cancer cell lines and showed mild anticancer activity (Ali et al. 2013). Besides, compounds with Schiff bases were reported to have antibacterial, anti-inflammatory, antioxidant and anticancer properties (Adams et al. 2013; Bhat et al. 2013). Because of the wide range of pharmacological activity exhibited by the Schiff bases, we envisaged developing a panel of noscapine derivatives in silico with substitution of Schiff bases, followed by screening the top three derivatives for chemical synthesis and experimental validation in a quest to increase the anticancer activity of noscapine. Due to its sensitive C–C bond, it is always challenging to synthesize noscapine derivatives. However, the reaction conditions embraced in this study do not influence the sensitive C–C bond connecting two heterocyclic phthalide and isoquinoline units. The synthetic derivatives and the lead molecule, noscapine were tested in vitro for their antiproliferative activity using two human cancer cell lines: MDA-MB-231 (a triple-negative human breast cancer cell line) and MCF-7 (a triple-positive human breast cancer cell line). The wide difference in IC_{50} values obtained using MCF-7 and MDA-MB-231 suggests that these compounds inhibited the cellular proliferation of cancer cells and were cell-type dependent. The 9-(*N*-arylmethylamino) derivatives of noscapine were found to have improved antiproliferative activity compared to noscapine and many of its synthetic derivatives reported earlier (Aneja et al. 2006b; Naik et al. 2011a; Manchukonda et al. 2013; Santoshi et al. 2011, 2015) without affecting the normal epithelial cells. These derivatives of noscapine were also found to arrest the cancer cell at G2/M phase and induced apoptosis to cancer cells quite effectively. This is corroborated from the previous study that many of the noscapine derivatives developed inhibited cell proliferation by interfering with cell cycle progression at G2/M phase (Anderson et al. 2005; Sajadian et al. 2015; Shen et al. 2015; Nagireddy et al. 2022; Devine

et al. 2018; Rahmanian-Devin et al. 2021). We have quantified the proportions of apoptotic cells (both early and late apoptotic cells) with the treatment of these derivatives using FACS analysis. Biochemically the apoptotic process is characterized by alterations of the lipid composition of cell membrane—phosphatidylserine which is normally on the inner leaflet of the cell membrane, translocates to the outer leaflet and is detected by annexin V binding. In contrast, a cell-impermeant DNA-binding fluorescent dye, propidium iodide, can only enter the cells at the late apoptosis stage when membrane permeability is compromised. The percentage of early apoptotic and late apoptotic cells using MDA-MB-231 cell line with the treatment of IC_{50} concentration of 9-(*N*-arylmethylamino) derivatives of noscapine were found to be significantly much higher compared to untreated cells (Fig. 9). Although the founding compound, noscapine, is already in clinical trials, 9-(*N*-arylmethylamino) derivatives of noscapine represents an additional edge over noscapine because of its higher potency, without compromising the nontoxic profile of noscapine.

Conclusion

A series of 9-(*N*-arylmethylamino) derivatives of noscapine were designed to enhance the activity of noscapine by functionalizing the C-9 position of noscapine with alkyl or arylalkyl units. When evaluated against MCF-7 & MDA-MB-231 cell line, the three screened noscapiniods showed a significant increase in the antiproliferative activity to cancerous cells without causing any harm to the normal cells. As a result, this class of compounds may be quite beneficial for treating breast cancer and different types of cancer. Thus this compels us to keep looking into the impacts of these new compounds in vivo animal research, with the ultimate goal of moving on to a human clinical trial.

Supplementary Information The online version contains supplementary material available at https://doi.org/10.1007/s13205-022-03445-3.

Acknowledgements We appreciate the financial assistance from the Government of India's ICMR (Grant No. 5/13/13/2019/NCD-III). We are appreciative of the additional facilities provided by Dr. Manu Lopus and the UM-DAE Centre for Excellence in Basic Sciences, Mumbai.

Funding We would like to thank the ICMR (Grant No. 5/13/13/2019/NCD-III), Government of India, for their financial assistance.

Data availability All data generated or analysed during this study are included in this published article (and its supplementary information files).

Declarations

Conflict of interests The authors declare no competing interests.

Compliance with Ethical Standards NA.

References

Adams M, Li Y, Khot H, De Kock C, Smith PJ, Land K, Chibale K, Smith GS (2013) The synthesis and antiparasitic activity of aryl- and ferrocenyl-derived thiosemicarbazone ruthenium (II)–arene complexes. Dalton Trans 42(13):4677–4685

Ali I, Haque A, Saleem K, Hsieh MF (2013) Curcumin-I Knoevenagel's condensates and their Schiff's bases as anticancer agents: synthesis, pharmacological and simulation studies. Bioorg Med Chem 21(13):3808–3820

Anderson JT, Ting AE, Boozer S, Brunden KR, Crumrine C, Danzig J, Dent T, Faga L, Harrington JJ, Hodnick WF, Murphy SM, Pawlowski G, Perry R, Raber A, Rundlett SE, Stricker-Krongrad A, Wang J, Bennani YL (2005) Identification of novel and improved antimitotic agents derived from noscapine. J Med Chem 48(23):7096–7098. https://doi.org/10.1021/jm050674q

Aneja R, Vangapandu SN, Lopus M, Chandra R, Panda D, Joshi HC (2006a) Development of a novel nitro-derivative of noscapine for the potential treatment of drug-resistant ovarian cancer and T-cell lymphoma. Mol Pharmacol 69(6):1801–1809. https://doi.org/10.1124/mol.105.021899

Aneja R, Vangapandu SN, Lopus M, Viswesarappa VG, Dhiman N, Verma A, Chandra R, Panda D, Joshi HC (2006b) Synthesis of microtubule-interfering halogenated noscapine analogs that perturb mitosis in cancer cells followed by cell death. Biochem Pharmacol 72(4):415–426

Aneja R, Dhiman N, Idnani J, Awasthi A, Arora SK, Chandra R, Joshi HC (2007a) Preclinical pharmacokinetics and bioavailability of noscapine, a tubulin-binding anticancer agent. Cancer Chemother Pharmacol 60(6):831–839. https://doi.org/10.1007/s00280-007-0430-y

Aneja R, Kalia V, Ahmed R, Joshi HC (2007b) Nonimmunosuppressive chemotherapy: EM011-treated mice mount normal T-cell responses to an acute lymphocytic choriomeningitis virus infection. Mol Cancer Ther 6(11):2891–2899. https://doi.org/10.1158/1535-7163.MCT-07-0359

Aneja R, Miyagi T, Karna P, Ezell T, Shukla D, Vij Gupta M, Yates C, Chinni SR, Zhau H, Chung LW, Joshi HC (2010) A novel microtubule-modulating agent induces mitochondrially driven caspase-dependent apoptosis via mitotic checkpoint activation in human prostate cancer cells. Eur J Cancer 46(9):1668–1678. https://doi.org/10.1016/j.ejca.2010.02.017

Becke A (1993) Density-functional thermochemistry. III the role of exact exchange. J Chem Phys 98:5648–5652

Bhardwaj VK, Das P, Purohit R (2022) Identification and comparison of plant-derived scaffolds as selective CDK5 inhibitors against standard molecules: Insights from umbrella sampling simulations. J Mol Liq 348:118015

Bhat MA, Al-Omar MA, Siddiqui N (2013) Antimicrobial activity of Schiff bases of coumarin-incorporated 1, 3, 4-oxadiazole derivatives: an in vitro evaluation. Med Chem Res 22(9):4455–4458

Binkley JS, Pople JA, Hehre WJ (1980) Self-consistent molecular orbital methods. 21. Small split-valence basis sets for first-row elements. J Am Chem Soc 102(3):939–947

Dahlström B, Mellstrand T, Löfdahl C-G, Johansson M (1982) Pharmakokinetic properties of noscapine. Eur J Clin Pharmacol 22(6):535–539

Devine SM, Yong C, Amenuvegbe D, Aurelio L, Muthiah D, Pouton C, Callaghan R, Capuano B, Scammells PJ (2018) Synthesis and pharmacological evaluation of noscapine-inspired 5-substituted tetrahydroisoquinolines as cytotoxic agents. J Med Chem 61(18):8444–8456

Friesner RA, Banks JL, Murphy RB, Halgren TA, Klicic JJ, Mainz DT, Repasky MP, Knoll EH, Shelley M, Perry JK, Shaw DE, Francis P, Shenkin PS (2004) Glide: a new approach for rapid, accurate docking and scoring. 1. Method and assessment of docking accuracy. J Med Chem 47(7):1739–1749. https://doi.org/10.1021/jm0306430

Gordon MS, Binkley JS, Pople JA, Pietro WJ, Hehre WJ (1982) Self-consistent molecular-orbital methods. 22. Small split-valence basis sets for second-row elements. J Am Chem Soc 104(10):2797–2803

Halgren TA, Murphy RB, Friesner RA, Beard HS, Frye LL, Pollard WT, Banks JL (2004) Glide: a new approach for rapid, accurate docking and scoring. 2. Enrichment factors in database screening. J Med Chem 47(7):1750–1759. https://doi.org/10.1021/jm030644s

Hamel E, Lin CM (1981) Glutamate-induced polymerization of tubulin: characteristics of the reaction and application to the large-scale purification of tubulin. Arch Biochem Biophys 209(1):29–40. https://doi.org/10.1016/0003-9861(81)90253-8

Jensen LN, Christrup LL, Jacobsen L, Bonde J, Bundgaard H (1992) Relative bioavailability in man of noscapine administered in lozenges and mixture. Acta Pharm Nord 4(4):309–312

Karlsson MO, Dahlstrom B, Eckernas SA, Johansson M, Alm AT (1990) Pharmacokinetics of oral noscapine. Eur J Clin Pharmacol 39(3):275–279. https://doi.org/10.1007/BF00315110

Ke Y, Ye K, Grossniklaus HE, Archer DR, Joshi HC, Kapp JA (2000) Noscapine inhibits tumor growth with little toxicity to normal tissues or inhibition of immune responses. Cancer Immunol Immunother 49(4–5):217–225. https://doi.org/10.1007/s002620000109

Krishna R, Mayer LD (2000) Multidrug resistance (MDR) in cancer: mechanisms, reversal using modulators of MDR and the role of MDR modulators in influencing the pharmacokinetics of anticancer drugs. Eur J Pharm Sci 11(4):265–283

Landen JW, Lang R, McMahon SJ, Rusan NM, Yvon AM, Adams AW, Sorcinelli MD, Campbell R, Bonaccorsi P, Ansel JC, Archer DR, Wadsworth P, Armstrong CA, Joshi HC (2002) Noscapine alters microtubule dynamics in living cells and inhibits the progression of melanoma. Cancer Res 62(14):4109–4114

Landen JW, Hau V, Wang M, Davis T, Ciliax B, Wainer BH, Van Meir EG, Glass JD, Joshi HC, Archer DR (2004) Noscapine crosses the blood-brain barrier and inhibits glioblastoma growth. Clin Cancer Res 10(15):5187–5201. https://doi.org/10.1158/1078-0432.CCR-04-0360

Lee C, Yang W, Parr RG (1988) Development of the Colle-Salvetti correlation-energy formula into a functional of the electron density. Phys Rev B 37(2):785

Manchukonda NK, Sridhar B, Naik PK, Joshi HC, Kantevari S (2012) Copper(I) mediated facile synthesis of potent tubulin polymerization inhibitor, 9-amino-alpha-noscapine from natural alpha-noscapine. Bioorg Med Chem Lett 22(8):2983–2987. https://doi.org/10.1016/j.bmcl.2012.02.033

Manchukonda NK, Naik PK, Santoshi S, Lopus M, Joseph S, Sridhar B, Kantevari S (2013) Rational design, synthesis, and biological evaluation of third generation α-noscapine analogues as potent tubulin binding anti-cancer agents. PLoS ONE 8(10):e77970

Manchukonda NK, Naik PK, Sridhar B, Kantevari S (2014) Synthesis and biological evaluation of novel biaryl type α-noscapine congeners. Bioorg Med Chem Lett 24(24):5752–5757

Mishra RC, Karna P, Gundala SR, Pannu V, Stanton RA, Gupta KK, Robinson MH, Lopus M, Wilson L, Henary M, Aneja R (2011) Second generation benzofuranone ring substituted noscapine analogs: synthesis and biological evaluation. Biochem Pharmacol 82(2):110–121. https://doi.org/10.1016/j.bcp.2011.03.029

Nagireddy PKR, Kumar D, Kommalapati VK, Pedapati RK, Kojja V, Tangutur AD, Kantevari S (2022) 9-Ethynyl noscapine induces G2/M arrest and apoptosis by disrupting tubulin polymerization in cervical cancer. Drug Dev Res 83(3):605–614. https://doi.org/10.1002/ddr.21888

Naik PK, Chatterji BP, Vangapandu SN, Aneja R, Chandra R, Kanteveri S, Joshi HC (2011a) Rational design, synthesis and biological evaluations of amino-noscapine: a high affinity tubulin-binding noscapinoid. J Comput Aided Mol Des 25(5):443–454. https://doi.org/10.1007/s10822-011-9430-4

Naik PK, Santoshi S, Rai A, Joshi HC (2011b) Molecular modelling and competition binding study of Br-noscapine and colchicine provide insight into noscapinoid–tubulin binding site. J Mol Graph Model 29(7):947–955

Naik PK, Lopus M, Aneja R, Vangapandu SN, Joshi HC (2012) In silico inspired design and synthesis of a novel tubulin-binding anti-cancer drug: folate conjugated noscapine (Targetin). J Comput Aided Mol Des 26(2):233–247

Oliva MA, Prota AE, Rodriguez-Salarichs J, Bennani YL, Jimenez-Barbero J, Bargsten K, Canales A, Steinmetz MO, Diaz JF (2020) Structural basis of noscapine activation for tubulin binding. J Med Chem 63(15):8495–8501. https://doi.org/10.1021/acs.jmedchem.0c00855

Panda D, Chakrabarti G, Hudson J, Pigg K, Miller HP, Wilson L, Himes RH (2000) Suppression of microtubule dynamic instability and treadmilling by deuterium oxide. Biochemistry 39(17):5075–5081. https://doi.org/10.1021/bi992217f

Pragyandipta P, Meher RK, Naik MR, Nagireddy PK, Pedapati RK, Kantevari S, Naik PK (2021) In-silico-inspired design of 1, 3-diynyl congeners of noscapine as promising tubulin-binding anticancer agent: chemical synthesis and cellular activity with breast cancer cell lines. ChemistrySelect 6(14):3500–3511

Rahmanian-Devin P, Baradaran Rahimi V, Jaafari MR, Golmohammadzadeh S, Sanei-Far Z, Askari VR (2021) Noscapine, an emerging medication for different diseases: a mechanistic review. Evid Based Complement Alternat Med 2021:8402517. https://doi.org/10.1155/2021/8402517

Sajadian S, Vatankhah M, Majdzadeh M, Kouhsari SM, Ghahremani MH, Ostad SN (2015) Cell cycle arrest and apoptogenic properties of opium alkaloids noscapine and papaverine on breast cancer stem cells. Toxicol Mech Methods 25(5):388–395. https://doi.org/10.3109/15376516.2015.1045656

Santoshi S, Naik PK, Joshi HC (2011) Rational design of novel anti-microtubule agent (9-azido-noscapine) from quantitative structure activity relationship (QSAR) evaluation of noscapinoids. J Biomol Screen 16(9):1047–1058. https://doi.org/10.1177/1087057111418654

Santoshi S, Manchukonda NK, Suri C, Sharma M, Sridhar B, Joseph S, Lopus M, Kantevari S, Baitharu I, Naik PK (2015) Rational design of biaryl pharmacophore inserted noscapine derivatives as potent tubulin binding anticancer agents. J Comput Aided Mol Des 29(3):249–270. https://doi.org/10.1007/s10822-014-9820-5

Sharma J, Bhardwaj VK, Purohit R (2021) Recognition of distinct chemical molecules as inhibitors for KIT receptor mutants D816H/Y/V: a simulation approach. J Mol Liq 339:116317

Shen W, Liang B, Yin J, Li X, Cheng J (2015) Noscapine increases the sensitivity of drug-resistant ovarian cancer cell line SKOV3/DDP to cisplatin by regulating cell cycle and activating apoptotic pathways. Cell Biochem Biophys 72(1):203–213. https://doi.org/10.1007/s12013-014-0438-y

Ye K, Ke Y, Keshava N, Shanks J, Kapp JA, Tekmal RR, Petros J, Joshi HC (1998) Opium alkaloid noscapine is an antitumor agent that arrests metaphase and induces apoptosis in dividing cells. Proc Natl Acad Sci USA 95(4):1601–1606. https://doi.org/10.1073/pnas.95.4.1601

Zhou R, Friesner RA, Ghosh A, Rizzo RC, Jorgensen WL, Levy R (2001) New linear interaction method for binding affinity calculations using a continuum solvent model. J Phys Chem B 105(42):10388–10397

Zhou J, Gupta K, Yao J, Ye K, Panda D, Giannakakou P, Joshi HC (2002) Paclitaxel-resistant human ovarian cancer cells undergo c-Jun NH2-terminal kinase-mediated apoptosis in response to noscapine. J Biol Chem 277(42):39777–39785. https://doi.org/10.1074/jbc.M203927200

Zhou J, Gupta K, Aggarwal S, Aneja R, Chandra R, Panda D, Joshi HC (2003) Brominated derivatives of noscapine are potent microtubule-interfering agents that perturb mitosis and inhibit cell proliferation. Mol Pharmacol 63(4):799–807. https://doi.org/10.1124/mol.63.4.799

Zhou J, Liu M, Aneja R, Chandra R, Lage H, Joshi HC (2006) Reversal of P-glycoprotein-mediated multidrug resistance in cancer cells by the c-Jun NH2-terminal kinase. Cancer Res 66(1):445–452. https://doi.org/10.1158/0008-5472.CAN-05-1779